Hindawi
Advances in Civil Engineering
Volume 2022, Article ID 1066833, 10 pages
https://doi.org/10.1155/2022/1066833

Research Article

Study on Evolution Law and the Mechanical Mechanism of Strong Mine Tremors in a Deep Coal Mine

Chao Wang,[1] Man Wang,[2] Siyuan Gong,[3] Junpeng Zou,[4] and Kunbo Wu[4]

[1]*Shandong Energy Group Co. Ltd., Jinan, Shandong 250014, China*
[2]*School of Information Engineering, Wuhan Business University, Wuhan 430056, China*
[3]*School of Mines, China University of Mining and Technology, Xuzhou, Jiangsu 221116, China*
[4]*Faculty of Engineering, China University of Geosciences, Wuhan, Hubei 430074, China*

Correspondence should be addressed to Kunbo Wu; wukunbo_cug@126.com

Received 25 July 2022; Accepted 11 October 2022; Published 12 November 2022

Academic Editor: Angelo Aloisio

Strong mine tremor occurs frequently in deep mines, which have brought great hidden dangers to the safety of mine production. This paper takes panel 63/06 in No. 6 mining area of Dongtan coal mine as the research background, through geological survey, laboratory test, theoretical analysis, numerical simulation, on-site microseismic monitoring, the seismic evolution law and its mechanical mechanism, etc., and the conclusions are as follows: (1) there are three sets of key layer groups between the surface of the panel 63/06 and the coal seam, among which there is a large amount of energy in the thick Jurassic red layer and the lower key layer, which provides an energy basis for the red-bed to break and generate strong mine tremors; (2) on the plane, most of the strong tremors occurred in front of the mining position of the working face and tended to transfer to the side of the gob, and longitudinal, high-energy mine tremors are mainly distributed in high-level red sandstone; (3) the release location of high-energy mining earthquakes does not match the location of microseismic accumulation, indicating that there is no elastic energy accumulation in the lower surrounding rock before the strong mining earthquake occurs, and it highlights the characteristics of structural occlusal instability rather than energy abrupt instability in the rupture of the red and thick sandstone; and (4) the Dongtan red-bed type strong mine tremors have a large focal rupture radius, a long rupture duration, a small corner frequency, and a weak initial *P* wave, and the characteristics of low stress drop and no catastrophic nature indicate that the thick and low-strength red-bed is prone to large-scale fractures, which should belong to the structural instability type mine shock dominated by tensile fracture.

1. Introduction

With the increase of mining depth, strong mine tremors induced by deep mining show a trend of increasing frequency and energy, which seriously restricts the normal safe production of mines and threatens the safety of underground miners and ground residents. The deep rock mass has the characteristics of high in-situ stresses, high temperature, high gas and water pressure under complex engineering geological conditions and harsh mechanical environments [1–3]. Strong tremors prevention and control management become the focus and difficulty of safe and efficient production in deep mines. A total of nearly 118 strong tremors are effectively located during the mining process in No.6 mining area of Dongtan coal mine. As of February 17, 2021, more than 20 strong tremor events have occurred at panel 63/06, which is being mined.

Thick and hard strata are developed during the formation of coal measure strata in East China [4, 5], among which thick-bedded sandstones (generally known as red-bed) are the most common ones. Tremors are triggered by the fracturing and violent movement of thick and hard strata [4, 6, 7]. Red-bed could form large hanging areas and cause higher stress concentrations above the coal seam under coal excavation. Based on key strata theory [8–10], thick and hard strata occur instantaneously and fracture and break to

release a large amount of elastic energy when the dynamic and static load of the overhanging position exceeds the critical stress. The key is to prevent the emergence of a large overhanging roof under the thick and hard rock strata structure because the occurrence of mine tremors is closely related to red-bed. So far, researchers have done lots of studies on the difficult challenge. To avoid or reduce strong mine tremors, hydraulic fracturing [11, 12], deep-hole blasting [13–15], nonpillar mining technologies are applied to break and weaken the roof [16–18] and have achieved a good effect in deep mines.

The mechanism of mine tremors and the prevention and control technology have been investigated by researchers. Based on the source location, energy, and waveform characteristics, seisms are categorized into three types: mining fracture, huge thick overburden, and high-energy vibration [19, 20]. Combined with the movement pattern of thick and hard rock strata, the roof motion tremors could be classified as fracture, return, and slip [21–23]. Research shows that the structural evolution of the overburden is closely related to the occurrence of mine seismicity [24–27]. Dou et al. [16, 28] made a study on the relationship between the evolution of overburden spatial structure and the occurrence law of mine seismicity and proposed the corresponding prevention and control measures according to different overburden structures. The risk of mine tremors occurrence is studied by Huang et al. [29], Xiao et al. [30], and Ju and Xu [31] through the fracture and energy accumulation-release characteristics of rock strata above the coal seam.

The mechanism for the occurrence of nonhazardous strong tremors induced by deep mining has not been clarified. It has been indicated that strong tremors do not cause damage to the roadway because they mostly occur in the goaf and its effective attenuation of vibration impact energy [32, 33]. From the waveforms recorded by the microseismic system, it could be shown that the strong mine tremor in Dongtan coal mine has a longer vibration duration, single main frequency component that is mainly low frequency, weak initial motion, low amplitude, and difficulty in localization compared with the impact rock burst signal. It is likely that the specificity of its red-bed sandstone fracture dynamics, rather than just the location of the seismic occurrence, determines the type of mine tremors [4, 34, 35]. In this paper, the characteristics of red-bed type strong tremors induced by deep mining are investigated, and the causes of frequent tremors are explained, and the induced mechanical mechanisms are revealed to provide theoretical guidance for the prevention and control of dynamic disasters in deep mines.

2. Engineering Background

Dongtan coal field with an area of 59.96 km^2 is located in the bordering area of Zoucheng, Yanzhou, and Qufu cities in Shandong Province, China. It is geologically located in the core and deep zone of the Yanzhou syncline. Currently, all mining activities are taking place at the first level (−660 m). The main mining coal seam is 3-coal-seam (3, 3 upper, and 3 lower), of which the 3upper coal seam has a buried depth of about 670 m with an average value of 5.41 m. Dongtan coal mine is divided into seven mining areas, and the No.6 mining area is located in the south of the coal mine. The stopped panels include the 63upper03 panel, 63upper04 panel, and 63upper05 panel in the No.6 mining area. The panel 63upper06 has been mined for 550 m.

The design track length of the panel 63upper06 is 1499 m, the transport length is 1489 m, the inclined width is 261 m, the elevation is −604.5 to −670.3 m, and the average is −637.4 m. The panel 63upper06 is mined on February 11, 2020. The division of panels is shown in Figure 1. Fully mechanized mining technology is adopted. The coal seam inclination is large in the west, with a maximum inclination of 14° at the starting cut and an overall average inclination of about 4°. The coal seam has a hardness of $f = 2 \sim 3$ on the Protodyakonov scale.

The geo-formation structure revealed by drill holes #170 and #O2-D7 within the range of panel 63upper06 is analysed statistically.As shown in Figure 2, three key layers can be identified between the surface and the coal seam, whose average thicknesses are 141 m, 217 m, and 30 m, and the distances from the coal seam are 331 m, 111 m, and 13 m, respectively. Key strata 2 and 3 are Jurassic sandstone layers and referred to as red-bed. Physical and mechanical tests find that key layer 1 is harder, with compressive strengths up to 88.2–127.5 MPa. However, the compressive strength of the red-bed ranges from 20 to 80 MPa, which is significantly weaker compared to the strength of the lower rock strata.

From the microseismic monitoring results during the mining process of panels in No.6 mining areas at the early stage, and it is known that the thickness of the red-bed in the area of frequent mine seismicity is 480 m ~ 520 m (see Figure 3). The distance between the red-bed and coal seam generally does not exceed 100 m. Therefore, the red-bed fractures instantaneously and releases a large amount of energy, resulting in strong tremors when the thickness of the red-bed increases and is close to the coal seam.

3. Stress Evolution and Energy Accumulation Characteristics of Overburden

3.1. Numerical Modeling. A three-dimensional numerical simulation model of deep mining in No.6 mining areas is constructed based on the principles of following the distribution of the goaf and the thickness and the physical and mechanical properties of rock strata. In Figure 4, the length, width, and height of the model are 2003 m, 1680 m, and 286 m, respectively. The stress evolution, degree of stress concentration, and energy accumulation characteristics of rock strata above the coal seam during the mining process of panel 63upper06 are calculated.

3.2. Stress Evolution and Energy Accumulation Characteristics of Panels. The panel 63upper06 has advanced 550.2 m. Panels 63upper03, 63upper04, and 63upper05 have been excavated. The existence of goafs will inevitably have a great impact on the stress distribution and energy accumulation in the panel [27, 36]. When the load on the overlying rock

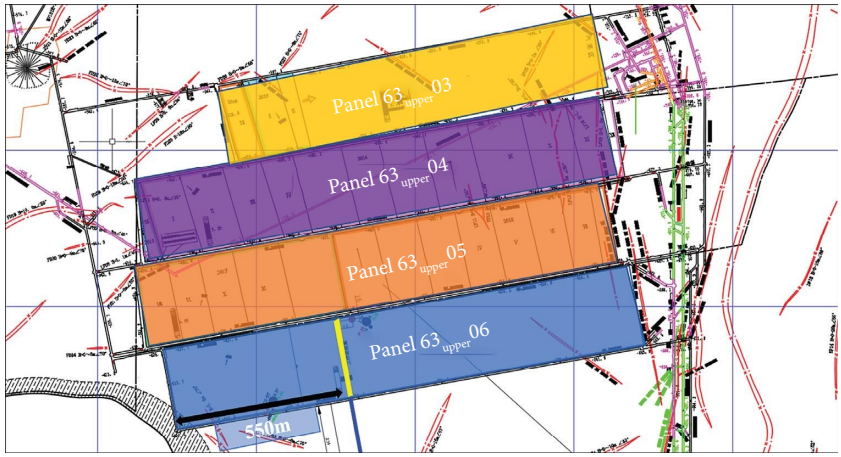

Figure 1: The division of panels in No.6 mining area.

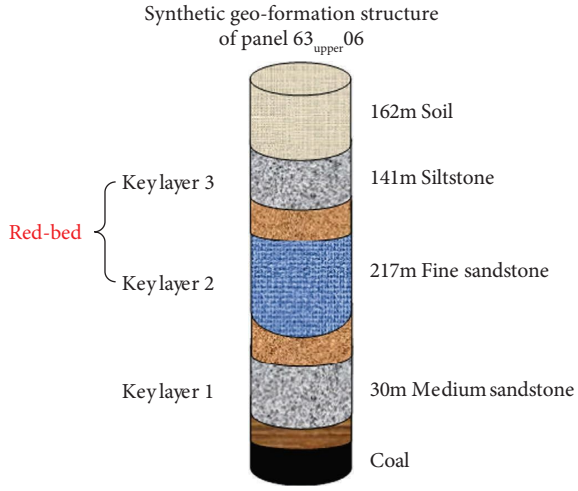

Figure 2: Analysis of key layers in the overburden above coal seam.

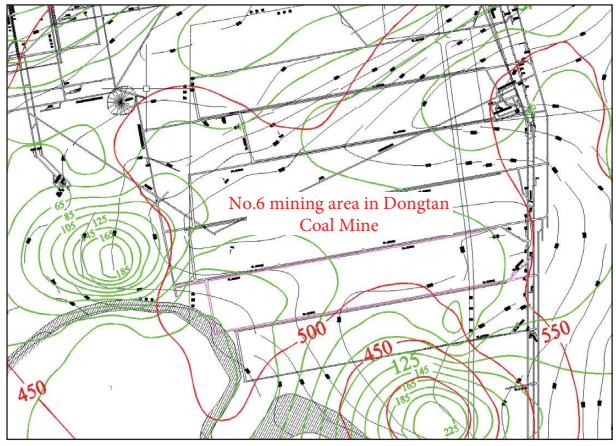

Figure 3: Distribution of the red-bed iso-thickness line (red), the red-bed bottom boundary, and the roof above coal seam iso-distance line (green).

strata exceeds its strength, the overburden collapses. In Figure 5, the maximum principal stress within the mining area is distributed within a limited range around the panel, and the maximum principal stress value has reached 68 MPa.

The maximum principal stress distribution in the coal seam and overlying strata during the continuation of the work face 63upper06 to 1350 m is analyzed. Figure 6 shows the evolution of the maximum principal stress along the

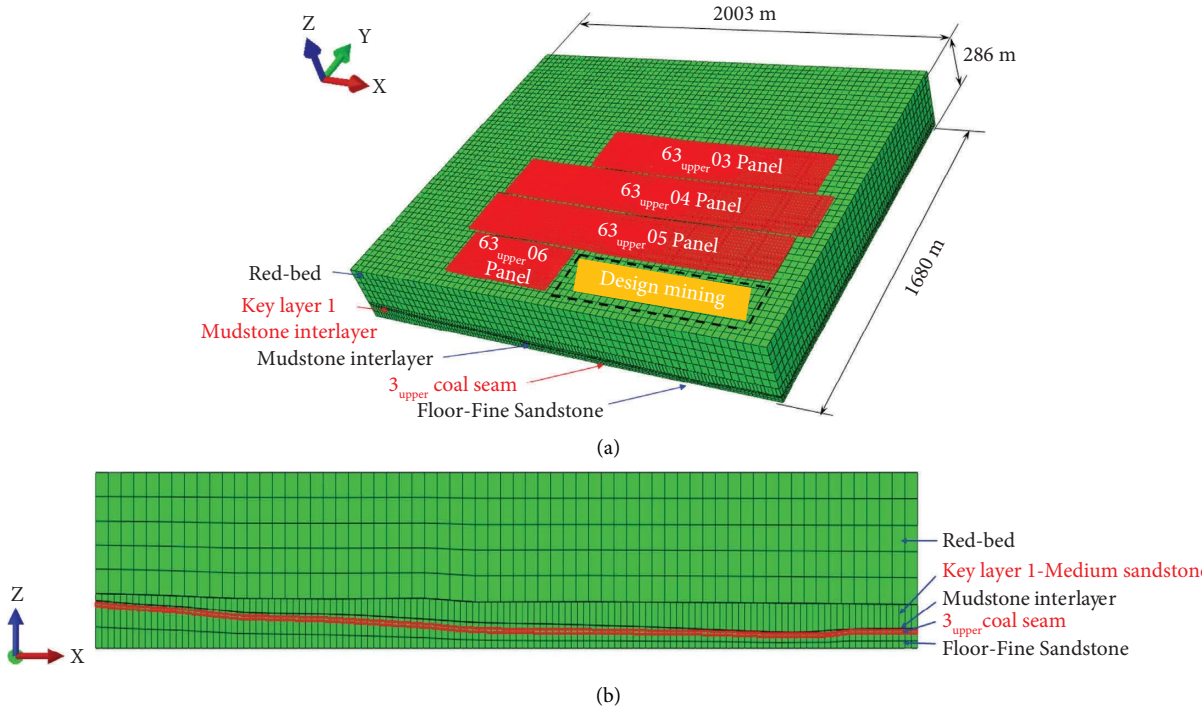

Figure 4: Numerical calculation model for overlying strata movement law in No.6 mining area. (a) 3D numerical simulation model. (b) Front view profile.

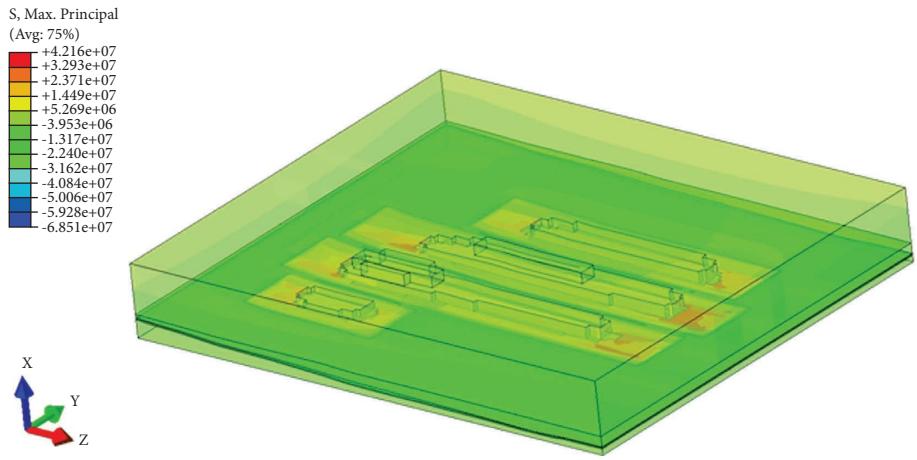

Figure 5: Maximum principal stress distribution in No.6 mining areas.

mining direction with the advancement of the working face. The distribution of the maximum principal stress in the spatial three-dimensional range of panel 63upper06 shows that the maximum principal stress value reaches 59.8 MPa. In Figure 7, the maximum principal stress in the current state of the working face 63upper06 up to about 650 m advance is at the highest value. The maximum principal stress tends to decrease during the subsequent advance. The working face advances to about 750 m to reach the lowest value, and then gradually rises.

As shown in Figure 8, a large amount of energy exists in the red-bed sandstone and key layers above the coal seam when the working face 63upper06 is advanced to 650 m, which provides an energy basis for generating strong mine tremors.

4. Study on Evolution Law of Strong Mine Tremors

4.1. Spatial Distribution Law of Strong Mine Tremors. A total of 25 strong mine tremors are effectively located on panel 63upper06 during the production period (Match 13, 2020 to November 30, 2020). After fine-tuning the *P*-wave initial arrival times of tremors, the distribution of strong mine tremors is obtained as shown in Figure 9. Tremors are mainly concentrated at a distance of approximately 230 to

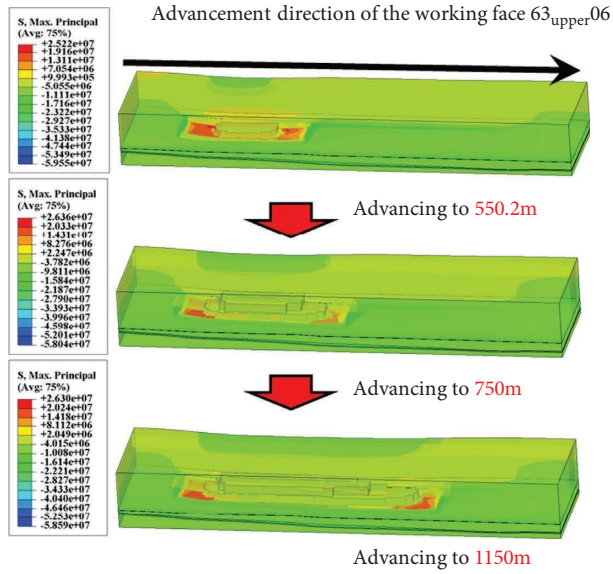

Figure 6: Cloud diagram of the maximum principal stress during the advance of the working face 63upper06.

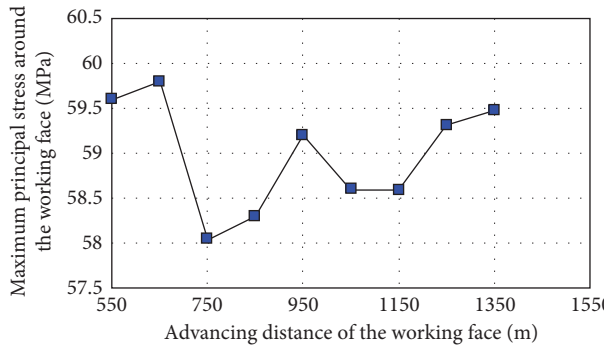

Figure 7: Relationship between the maximum principal stress around the working face and the advancing distance.

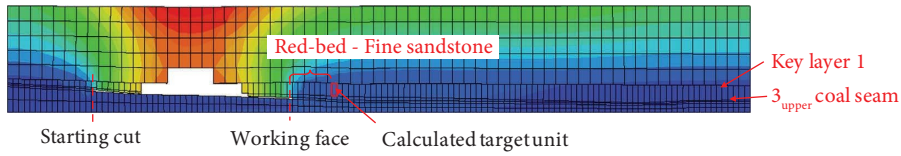

Figure 8: Schematic diagram of target element for calculating strain energy.

489 m from the starting cut, roughly in the area between 1st square and 2nd square.

Strong mine tremors mainly occur in the 300 m range before and after the working face (see Figure 10). With the gradual advancement of the working face, most tremors occur in front of the working face and are in a fluctuating state, except for the first strong tremor which occurs behind the starting cut of the panel. With mining, strong mine tremors occur first at positions far from the extraction location, gradually approaching the working face, and then transferring to the front of the working face. Overall, there is a tendency for strong mine tremors to shift to the side of the goaf. It indicates that strong mine tremors at panel 63upper06 are influenced by the overburden structure.

In Figure 11, large-energy mine tremors are mostly distributed in key layers 2 and 3 from the spatial distribution of tremors. Considering factors such as the thinness of key layer 1 and the influence of locating accuracy, there are fewer mine tremors occurring directly in key layer 1. The great majority of strong mine tremors have a low impact on mine safety production. Therefore, it could be verified that strong mine tremors occurring in key layers 2 and 3 are not

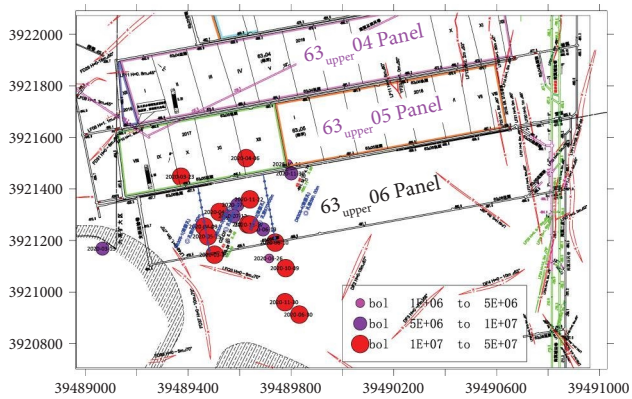

Figure 9: Plan of strong mine tremors distribution.

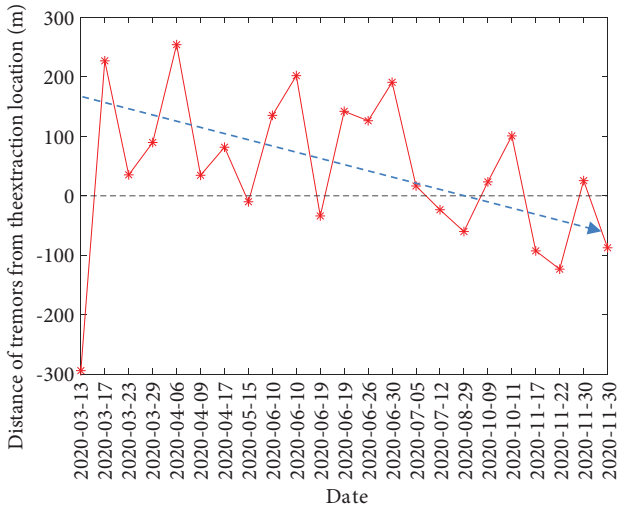

Figure 10: The curve of strong mine tremors relationship with extraction location.

significant in terms of inducing disasters, but they will cause strong shocks on the ground. Meanwhile, large-energy mine seismic signals are also monitored at lower rock strata. Take the strong mine seismic signal that occurred on November 30, 2020, at 09:41:29 as an example. The error calculation shows that its Z-direction elevation error is 46.8 m. After correction, it should be located in key layer 1 in spatial position.

Strong mine tremors at panel 63upper06 have a tendency to develop from far-field strata to lower rock strata. After the fracture of key layers, several strong mine tremors will accompany the lower strata [4, 28, 37]. The fracture of far-field strata will be acting as a load directly on the near-field strata, which is extremely negative for the normal break of the lower layers, especially for key layer 1 [38–40]. The energy released by the breakage of near-field rock strata immediately is applied to the coal seam and has greater disaster-causing effects than far-field strata because it is closer to the coal seam and has higher strength. Therefore, it can be inferred from the above analysis that it is more important to treat the lower rock strata than the higher ones.

4.2. Characteristics of Strong Mine Tremors Energy Release. Figure 12 shows the statistical curves of mine seismic energy and also frequency and extraction location at panel 63upper06 from February 15, 2020, to November 29, 2020. The large-energy mine tremors are mostly in the form of single peaks, indicating that the strong tremors at panel 63upper06 have an individual character in Figure 12(a). There are no significant energy and frequency changes in the source area and the surrounding area before and after the occurrence of strong tremors, reflecting more structural occlusion instability than instantaneous energy unsteadiness.

Strong tremors mainly occur in a range of 540 m in front and behind the working face, which could affect up to 300 m area in the direction of advancement and 240 m area in the direction of the goaf. However, the unfavorable case is that large-energy tremors occur near the extraction location of the working face during the statistical time period, which increases the risk of induced rock burst of disaster-causing mine seisms.

The distribution law of the frequency and energy of mine tremors in panel 63upper06 is shown in Figure 12(b) after eliminating large-energy tremors (>105 J). It could be seen that there is a strong consistent frequency curve and energy curve, which is similar to the trend of most mine regulations. The statistical analysis of tremors in Dongtan coal mine shows that large-energy seisms mostly occur in higher strata, and small-energy seisms mainly occur in lower strata above coal seams. The peak of the effect of the lower strata superelevation is approximately at the position of 130 m, which is the main area of concentrated mine seismic release, and the farthest location that can be affected is 370 m.

As a result, strong mine tremors caused by the breakage of the high-level roof at panel 63upper06 and small-energy seisms occurring within the lower roof and coal are released in two different types of energy. Strong tremors are distributed both in front and behind the working face, while small-energy seisms are mainly distributed in front of the working face. Considering the correlation between the far-field rock strata and the near-field strata breakage, the comprehensive determination of panel 63upper06 mining supervision could have an influence on the range of about 350 m.

5. Study on the Mechanical Mechanism of Strong Mine Tremors

It is generally believed that the harder the rock strata the more difficult it is to fracture, but the breakage frequency of red-bed sandstone is significantly higher. On the other hand, it means that the overlying high red-bed is easier to be fractured with the mining of No.6 mining area, which will result in the high-energy mine tremors phenomenon. The reason is that the red-bed is not hard but strong integrity and large thickness exist in a close relationship. As shown in Figure 13, most of the strong tremors that occurred in No.6 mining area of Dongtan coal mine are low-frequency-type seisms. The average dominant frequency of strong mine tremors at panel 63upper06 is found to be 2–4 Hz after statistical analysis of the waveform of 25 seismic events. The

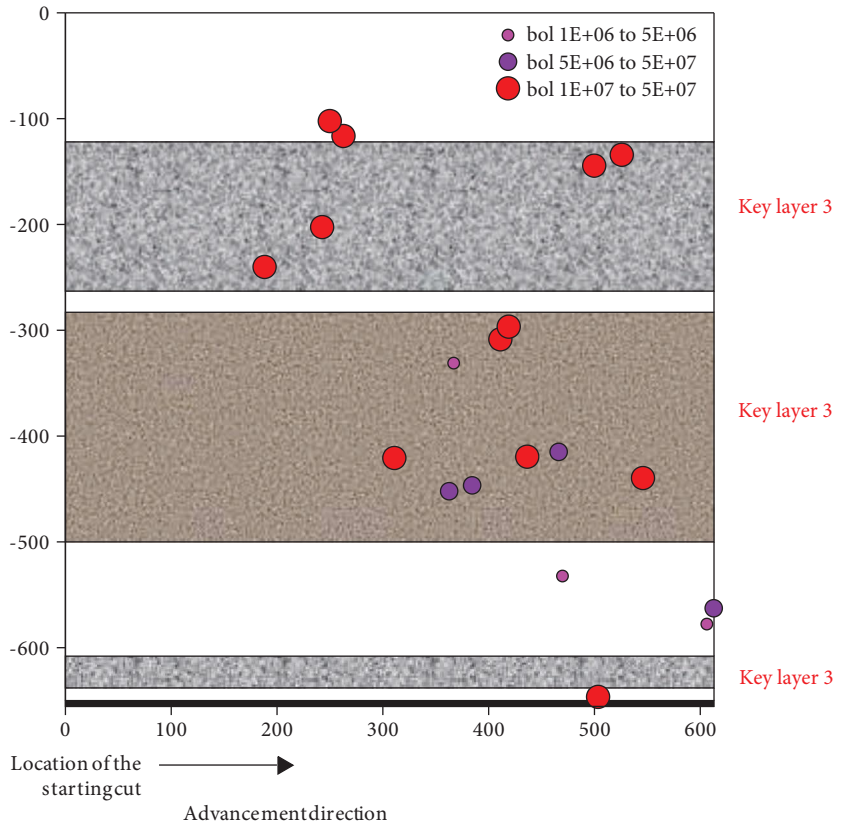

Figure 11: Profile of the location of strong mine tremors at panel 63upper06.

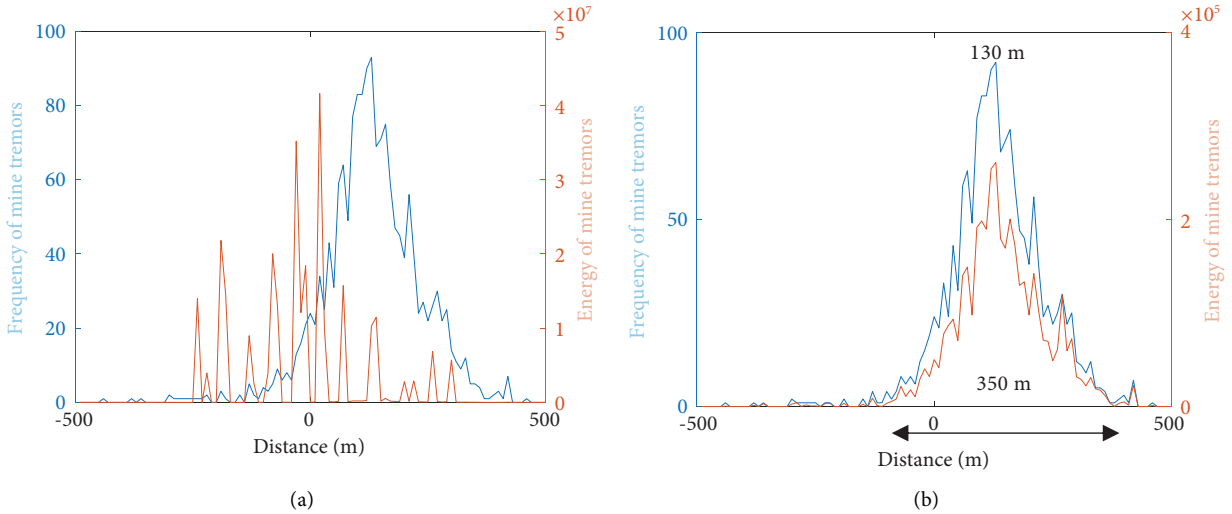

Figure 12: The distribution law of mine tremors near the extraction location of panel 63upper06. (a) Statistical results including all mine tremors. (b) Statistical results after eliminating mine tremors over 10^5 J.

waveform signal is commonly characterized by the long fracture duration and less over-range, reflecting the weak disaster-causing feature of strong tremors.

To further analyze and determine the mechanism of strong tremor occurrence, the seismic signal in Figure 13 is used as an example, and its source parameters are calculated by geophysical methods (e.g., seismic moment, corner frequency, circular source radius, and stress drop) [41–44]. It could be seen that the longer the duration of seismic fracture, the larger the circular source radius, and the smaller the stress drop, which is the primary reason for the weak effect of rock burst induced by strong red-bed type mine tremors. By

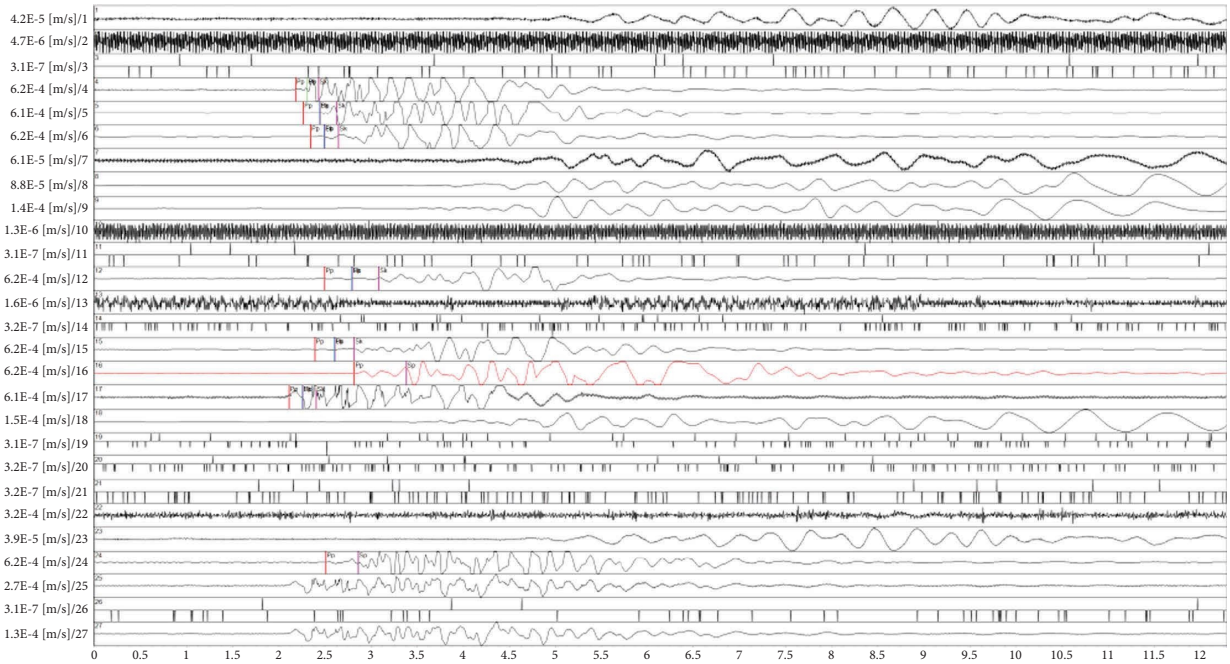

Figure 13: Recording of strong tremor signals on November 30, 2020, at 09:41:49.

Table 1: Results of seismic source parameters solution.

Date	Circular source radius (m)	Corner frequency (Hz)	Seismic moment (N·m)	Seism magnitude	Stress drop (MPa)	Fracture duration (s)
2020-11-30 09.41.49	150	2.98	$9.07E+11$	1.97	0.12	0.34

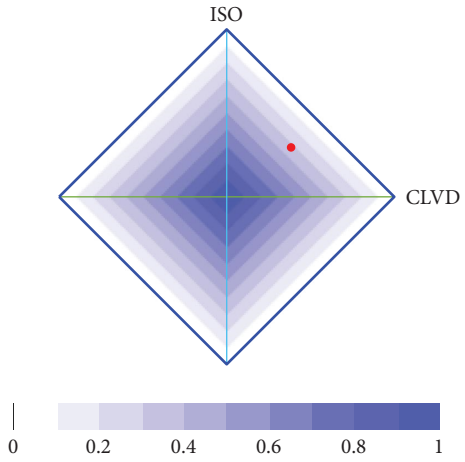

Figure 14: The focal mechanism solution results of the strong mine tremor on November 30, 2020, at 09:41:49.

comprehensive analysis of p-wave initial motion signals recorded by 25 seisms, it is revealed that the weak initial motion of red-bed type seismic signals is consistent with the low stress drop. The results indicate that red-bed type strong mineral seismicity may not require a high stress environment to be generated. The preliminary inference is that it belongs to the red-bed structural instability type mine tremor. The released energy originates mainly from the gravitational potential energy of the red-bed (Table 1).

Based on the moment tensor inversion method to analyze the focal mechanism [41, 45, 46], the solution results are given in Figure 14. The results show that the red-bed mine tremor contains both shear-fracturing and tensile-fracturing components, and the comprehensive performance is a mixed fracturing mechanism dominated by tensile failure.

6. Conclusions

The mechanical mechanism of strong mine tremors is not clarified under the mining of deep coal seam. In this paper, based on numerical simulation, on-site microseismic monitoring, and moment tensor inversion, the spatial distribution characteristic and mechanical mechanism of mine tremors as well as the evolution law of overburden stress are revealed. The following conclusions can be drawn:

(1) Three key layers could be determined between the surface and coal seam by comprehensive analysis of the stratigraphic structure in No.6 mining area of Dongtan coal mine. The numerical simulation results

indicate that a large amount of energy is accumulated in the thick and hard rock strata above the coal seam, which provides the energy basis for the rock layer fracture to generate strong mine tremors.

(2) Most of strong mine tremors occur in front of the extraction location at the panel, and there is a tendency to transfer to the goaf. It shows that the strong seism at panel 63upper06 is dominantly affected by the local area overburden structure. Meanwhile, large-energy mine tremors are concentrated in the high-level key layer, but a little occurs in the lower key layer.

(3) Mismatch between the position of high-energy mine seismic release and microseismic accumulation is seen by analyzing the distribution of high-energy and low-energy mine tremors as the working face extraction. It means that there is no elastic energy accumulation in the lower surrounding rock mass before the occurrence of strong mine tremors. It highlights that the red-bed breakage presents structural occlusion instability rather than instantaneous energy unsteadiness, which brings great difficulties to the early warning of large-energy seisms.

(4) The red-bed type strong mine tremor has the characteristics of large circular source radius, long fracture duration, small corner frequency, weak p-wave initial motion, low stress drop, and no disaster-causing property in Dongtan coal mine. This suggests that the huge thick and low-strength red-bed is easily fractured on the large scale. Seism events belong to the strong mine tremor of structural instability dominated by tensile failure.

Data Availability

The datasets generated during and/or analyzed during the current study are available from the corresponding author on reasonable request.

Conflicts of Interest

The authors declare that they have no conflicts of interest.

References

[1] P. G. Ranjith, J. Zhao, M. H. Ju, R. V. D. Silva, T. D. Rathnaweera, and A. K. Bandara, "Opportunities and challenges in deep mining: a brief review," *Engineering*, vol. 3, pp. 546–551, 2017.

[2] H. P. Xie, M. Z. Gao, R. Zhang, G. Y. Peng, W. Y. Wang, and A. Q. Li, "Study on the mechanical properties and mechanical response of coal mining at 1000 m or deeper," *Rock Mechanics and Rock Engineering*, vol. 52, no. 5, pp. 1475–1490, 2019.

[3] H. P. Xie, C. Li, Z. Q. He et al., "Experimental study on rock mechanical behavior retaining the in situ geological conditions at different depths," *International Journal of Rock Mechanics and Mining Sciences*, vol. 138, Article ID 104548, 2021.

[4] Y. Y. Jiao, K. B. Wu, J. P. Zou et al., "On the strong earthquakes induced by deep coal mining under thick strata-a case study," *Geomechanics and Geophysics for Geo-Energy and Geo-Resources*, vol. 7, no. 4, p. 97, 2021.

[5] P. F. Lyu, J. B. Lu, E. Y. Wang, and X. H. Chen, "The mechanical criterion of activation and instability of normal fault induced by the movement of key stratum and its disaster-causing mechanism of rockburst in the hanging wall mining," *Advances in civil engineering*, vol. 2021, Article ID 6618957, 11 pages, 2021.

[6] C. Xu, Q. Fu, X. Y. Cui, K. Wang, Y. X. Zhao, and Y. B. Cai, "Apparent-depth effects of the dynamic failure of thick hard rock strata on the underlying coal mass during underground mining," *Rock Mechanics and Rock Engineering*, vol. 52, no. 5, pp. 1565–1576, 2019.

[7] M. L. Yu, J. P. Zuo, Y. J. Sun, C. N. Mi, and Z. D. Li, "Investigation on fracture models and ground pressure distribution of thick hard rock strata including weak interlayer," *International Journal of Mining Science and Technology*, vol. 32, pp. 137–153, 2022.

[8] L. X. Wu, M. G. Qian, and J. Z. Wang, "The influence of a thick hard rock stratum on underground mining subsidence," *International Journal of Rock Mechanics and Mining Sciences*, vol. 34, pp. 341–344, 1997.

[9] M. G. Qian, X. X. Miao, J. L. Xu, and X. B. Mao, *Key Strata Theory in Ground Control,* China University of Mining and Technology Press, Xuzhou, China, 2000.

[10] Y. Y. Lu, T. Gong, B. W. Xia, B. Yu, and F. Huang, "Target stratum determination of surface hydraulic fracturing for far-field hard roof control in underground extra-thick coal extraction: a case study," *Rock Mechanics and Rock Engineering*, vol. 52, no. 8, pp. 2725–2740, 2019.

[11] B. X. Huang, Y. Z. Wang, and S. G. Cao, "Cavability control by hydraulic fracturing for top coal caving in hard thick coal seams," *International Journal of Rock Mechanics and Mining Sciences*, vol. 74, pp. 45–57, 2015.

[12] J. Zou, Y. Y. Jiao, F. Tan, J. Lv, and Q. Zhang, "Complex hydraulic-fracture-network propagation in a naturally fractured reservoir," *Computers and Geotechnics*, vol. 135, Article ID 104165, 2021.

[13] P. Gong, Y. H. Chen, Z. G. Ma, and S. X. Cheng, "Study on stress relief of hard roof based on presplitting and deep hole blasting," *Advances in Civil Engineering*, vol. 2020, Article ID 8842818, 12 pages, 2020.

[14] G. F. Wang, S. Y. Gong, L. M. Dou, W. Cai, X. Y. Yuan, and C. J. Fan, "Rockburst mechanism and control in coal seam with both syncline and hard strata," *Safety Science*, vol. 115, pp. 320–328, 2019.

[15] X. P. Lai, C. Jia, F. Cui et al., "Microseismic energy distribution and impact risk analysis of complex heterogeneous spatial evolution of extra-thick layered strata," *Scientific Reports*, vol. 12, no. 1, Article ID 10832, 2022.

[16] L. M. Dou, C. P. Lu, Z. L. Mu, and M. S. Gao, "Prevention and forecasting of rock burst hazards in coal mines," *Mining Science and Technology*, vol. 19, pp. 585–591, 2009.

[17] X. Y. Liu, M. C. He, J. Wang, and Z. M. Ma, "Research on non-pillar coal mining for thick and hard conglomerate roof," *Energies*, vol. 14, pp. 299–312, 2021.

[18] G. L. Zhu, R. L. Sousa, M. C. He, P. Zhou, and J. Yang, "Stability analysis of a non-pillar-mining approach using a combination of discrete fracture network and discrete-element method modeling," *Rock Mechanics and Rock Engineering*, vol. 53, no. 1, pp. 269–289, 2020.

[19] G. Mutke, A. Lurka, and Z. Zembaty, ""Prediction of rotational ground motion for mining-induced seismicity – case study from upper silesian coal basin, Poland", engineering

geology," *Engineering Geology*, vol. 276, Article ID 105767, 2020.

[20] C. P. Lu, G. J. Liu, Y. Liu, N. Zhang, J. H. Xue, and L. Zhang, "Microseismic multi-parameter characteristics of rockburst hazard induced by hard roof fall and high stress concentration," *International Journal of Rock Mechanics and Mining Sciences*, vol. 76, pp. 18–32, 2015.

[21] M. J. Mendecki, J. Szczygieł, G. Lizurek, and L. Teper, "Mining-triggered seismicity governed by a fold hinge zone: the upper silesian coal basin, Poland," *Engineering geology, Engineering Geology*, vol. 274, Article ID 105728, 2020.

[22] Z. L. He, C. P. Lu, X. F. Zhang, Y. Guo, Z. H. Meng, and L. Xia, "Numerical and field investigations of rockburst mechanisms triggered by thick-hard roof fracturing," *Rock Mechanics and Rock Engineering*, 2022.

[23] S. L. Wang, G. L. Zhu, K. Z. Zhang, and L. Yang, "Study on characteristics of mining earthquake in multicoal seam mining under thick and hard strata in high position", shock and vibration," *Shock and Vibration*, vol. 55, pp. 6863–6886, Article ID 6675089, 2021.

[24] A. Y. Cao, L. M. Dou, W. Cai, S. Y. Gong, S. Liu, and G. C. Jing, "Case study of seismic hazard assessment in underground coal mining using passive tomography," *International Journal of Rock Mechanics and Mining Sciences*, vol. 78, pp. 1–9, 2015.

[25] K. Ma, S. J. Wang, F. Z. Yuan, Y. L. Peng, S. M. Jia, and F. Gong, "Study on mechanism of influence of mining speed on roof movement based on microseismic monitoring," *Advances in Civil Engineering*, vol. 2020, Article ID 8819824, 9 pages, 2020.

[26] C. Zhou, S. T. Zhu, D. Z. Song, F. X. Jiang, J. H. Liu, and J. J. Li, "Study on the mechanism of repeated mining tremor in multiple key layers: a typical case study," *Geotechnical & Geological Engineering*, vol. 40, no. 10, pp. 5139–5151, 2022.

[27] L. M. Dou and H. He, "Studyof OX-F-T spatial structure evolutionof overlying StratainCoal mines," *Chinese journal of rock mechanics and engineering*, vol. 31, pp. 453–460, 2012.

[28] H. He, L. M. Dou, A. Y. Cao, and J. Fan, "Mechanisms of mining seismicity under large scale exploitation with multikey strata", shock and vibration," *Shock and Vibration*, vol. 2015, Article ID 313069, 9 pages, 2015.

[29] G. J. Huang, J. Ba, Q. Z. Du, and J. M. Carcione, "Simultaneous inversion for velocity model and microseismic sources in layered anisotropic media," *Journal of Petroleum Science and Engineering*, vol. 173, pp. 1453–1463, 2019.

[30] Y. X. Xiao, X. T. Feng, J. A. Hudson, B. R. Chen, G. L. Feng, and J. P. Liu, "ISRM suggested method for in situ microseismic monitoring of the fracturing process in rock masses," *Rock Mechanics and Rock Engineering*, vol. 49, no. 1, pp. 343–369, 2016.

[31] J. F. Ju and J. L. Xu, "Structural characteristics of key strata and strata behaviour of a fully mechanized longwall face with 7.0m height chocks," *International Journal of Rock Mechanics and Mining Sciences*, vol. 58, pp. 46–54, 2013.

[32] L. H. Wang, A. Y. Cao, L. M. Dou et al., "Numerical simulation on failure effect of mining-induced dynamic loading and its influential factors," *Safety Science*, vol. 113, pp. 372–381, 2019.

[33] S. Q. He, D. Z. Song, Z. L. Li et al., "Precursor of spatio-temporal evolution law of MS and AE activities for rock burst warning in steeply inclined and extremely thick coal seams under caving mining conditions," *Rock Mechanics and Rock Engineering*, vol. 52, no. 7, pp. 2415–2435, 2019.

[34] A. Y. Cao, L. M. Dou, W. Cai, S. Y. Gong, S. Liu, and Y. L. Zhao, "Tomographic imaging of high seismic activities in underground island longwall face," *Arabian Journal of Geosciences*, vol. 9, no. 3, p. 232, 2016.

[35] K. Ma, F. Z. Yuan, H. B. Wang et al., "Fracture mechanism of roof key strata in Dongjiahe coal mine using microseismic moment tensor," *Geomatics, Natural Hazards and Risk*, vol. 12, pp. 1467–1487, 2021.

[36] B. Yu, Z. Y. Zhang, T. J. Kuang, and J. R. Liu, "Stress changes and deformation monitoring of longwall coal pillars located in weak ground," *Rock Mechanics and Rock Engineering*, vol. 49, no. 8, pp. 3293–3305, 2016.

[37] D. Mondal, P. N. S. Roy, and M. Kumar, "Monitoring the strata behavior in the Destressed Zone of a shallow Indian longwall panel with hard sandstone cover using Mine-Microseismicity and Borehole Televiewer data," *Engineering Geology*, vol. 271, Article ID 105593, 2020.

[38] T. J. Kuang, Z. Li, W. B. Zhu et al., "The impact of key strata movement on ground pressure behaviour in the Datong coalfield," *International Journal of Rock Mechanics and Mining Sciences*, vol. 119, pp. 193–204, 2019.

[39] B. F. An, X. X. Miao, J. X. Zhang, F. Ju, and N. Zhou, "Overlying strata movement of recovering standing pillars with solid backfilling by physical simulation," *International Journal of Mining Science and Technology*, vol. 26, pp. 301–307, 2016.

[40] Z. K. Yang, Z. H. Cheng, Z. H. Li et al., "Movement laws of overlying strata above a fully mechanized coal mining face backfilled with gangue: a case study in jiulishan coal mine in henan Province, China," *Advances in Civil Engineering*, vol. 202120 pages, 2021.

[41] J. N. Brune, ""Tectonic stress and the spectra of seismic shear waves from earthquakes", Journal of Geophysical Research: solid Earth," *Journal of Geophysical Research*, vol. 75, pp. 4997–5009, 1970.

[42] K. Aki and H. Patton, "Determination of seismic moment tensor using surface waves," *Tectonophysics*, vol. 49, pp. 213–222, 1978.

[43] T. C. Hanks and H. Kanamori, ""A moment magnitude scale", journal of geophysical research: solid earth," *Journal of Geophysical Research*, vol. 84, pp. 2348–2350, 1979.

[44] G. Calderoni, A. Rovelli, and R. D. Giovambattista, "Stress drop, apparent stress, and radiation efficiency of clustered earthquakes in the nucleation volume of the 6 mw 6.1 L'aquila earthquake," *journal of geophysical research: solid earth*, vol. 124, pp. 10360–10375, 2019.

[45] M. Kozłowska, B. Orlecka-Sikora, Ł. Rudziński, S. Cielesta, and G. Mutke, "Atypical evolution of seismicity patterns resulting from the coupled natural, human-induced and coseismic stresses in a longwall coal mining environment," *International Journal of Rock Mechanics and Mining Sciences*, vol. 86, pp. 5–15, 2016.

[46] J. Ma, L. J. Dong, G. Y. Zhao, and X. B. Li, "Discrimination of seismic sources in an underground mine using full waveform inversion," *International Journal of Rock Mechanics and Mining Sciences*, vol. 106, pp. 213–222, 2018.